Hydrology & Water Resources Symposium
12-15 November | Sydney

ENGINEERS AUSTRALIA | National Committee on Water Engineering

**ISBN number for HWRS 2023 is 978-1-925627-81-7**

# Reynolds Stresses and Secondary Motion in Box Culvert Barrel: Implications in terms of Upstream Fish Passage at Road Crossings

Hui Ling Wong

The University of Queensland, School of Civil Engineering, Brisbane QLD 4972, Australia

huiling.wong@uq.net.au

Hubert Chanson

The University of Queensland, School of Civil Engineering, Brisbane QLD 4972, Australia

h.chanson@uq.edu.au

## ABSTRACT

*A culvert is a covered channel designed to pass water through an embankment. The adverse ecological impacts of road crossings on upstream fish passage has driven the development of new culvert design guidelines with a focus on small-bodied native fish species and juveniles of larger fish. Previous literatures focused on the usage of baffles and macro-roughness, although these can drastically reduce the discharge capacity of the culvert. Such approaches have raised concerns in relation to the total costs of these structures. Hence, new research was carried out with the aim of developing fish friendly box culverts without altering the design capacity. The study focused on the low velocity zones conducive of upstream fish passage. Detailed turbulence measurements were undertaken in a near full-scale box culvert barrel. Velocity and Reynolds stress measurements showed some strong secondary motion of Prandtl's second kind. The channel boundaries and bottom corners contributed to the occurrence of low-velocity zones. The characteristics of these low-velocity zones were carefully detailed. The results demonstrated how the bottom corners in standard box culvert barrel can induce a strong flow three-dimensionality, conducive of successful upstream passage of small-bodied fish.*

## INTRODUCTION

The movements of fishes in natural streams are impacted by in-stream man-made structures, including road crossings and weirs (Warren and Pardew 1998; Anderson et al. 2012; Baumgartner et al. 2012). These may prevent or reduce fish passage and cause fish mortalities and injuries. Fishes display a wide range of biological adaptations linked to a broad variety of swimming techniques and performances in response to different natural and man-made environment (Behlke et al. 1991; Mallen-Cooper 1996; Olsen and Tullis 2013). The challenge in developing fish-friendly road crossings is knowing exactly what the water is doing where the fish swims and what the resulting hydrodynamic interactions are. In this study, small-bodied fish are defined as fish with body length lesser than 120 mm. With small-bodied fish and juvenile of larger fish, the upstream traversability of the culvert barrel (Fig. 1) is a massive obstacle, because of the high water velocities.

A number of field observations and near-full-scale prototype experiments demonstrated that small fish predominantly swim upstream next to the bottom corners and sidewalls of box culvert barrel (Cahoon et al. 2007; Blank 2008; Jensen 2014; Wang et al. 2016; Cabonce et al. 2019). The fishes use low-velocity zones (LVZs) as preferential swimming zones (Fig. 2). Recent detailed physical and numerical CFD modelling characterised the geometric dimensions of these LVZs in standard box culverts (Sailema et al. 2020; Leng and Chanson 2020, 2020b). Sailema et al. (2020) utilised different corner baffles configurations to manipulate the LVZ zone. On the other hand, Leng and Chanson (2020b) used hybrid modelling to characterised LVZ in different flow condition but without insights of the hydrodynamic conditions in LVZ. Yet the hydrodynamic motion in a box culvert barrel leads to a complicated fluid dynamics. The strongest turbulence is generated in the corner regions with their effects seen in most parts of the channel (Prandtl 1952; Chanson 2019). Secondary currents develop as a result of the hydrodynamic singularities generated by the corners (Fig. 2) and are associated with large turbulent Reynolds stresses next to the singularities.

It is the aim of this study to characterise the complex turbulent flow motion in the low velocity zones which are preferential swimming zones of small-bodied fish. This was achieved through some physical modelling in a near-full-scale laboratory facility under controlled flow conditions.

**Figure 1. Standard box culvert structures. Left: outlet of 2 cells box culvert on Cubberla Creek, Kenmore QLD (Australia); Right: outlet of multicell box culvert along Coolaba Creek, Yeerongpilly QLD (Australia)**

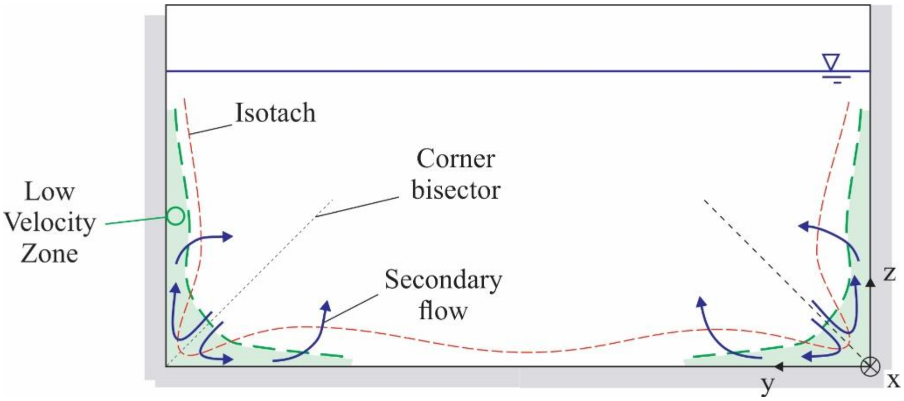


**Figure 2. Secondary circulation of Prandtl's second kind in a box culvert barrel - Green shades highlight the low-velocity zones**

## METHODS, FACILITY AND INSTRUMENTATION

The new laboratory experiments were conducted in a 15 m long 0.5 m wide horizontal rectangular channel (Fig. 3). The invert of the flume was some smooth PVC and the sidewalls were in tempered glass. The relatively-large-size flume acted at a near-full-scale single-box culvert barrel. The results' extrapolation to larger culvert structures would be based upon a joint Froude and Morton similarity. The geometric scaling ratio would range from 1:1 to 1:4 for typical precast concrete boxes between 0.5

m and 2 m in width. The water was supplied by a constant head reticulation system feeding a 2.0 m long 1.25 m wide intake basin, equipped with baffles, flow straighteners and three-dimensional convergent section leading to the 0.5 m wide flume. The flume ended with a free overfall at the downstream end.

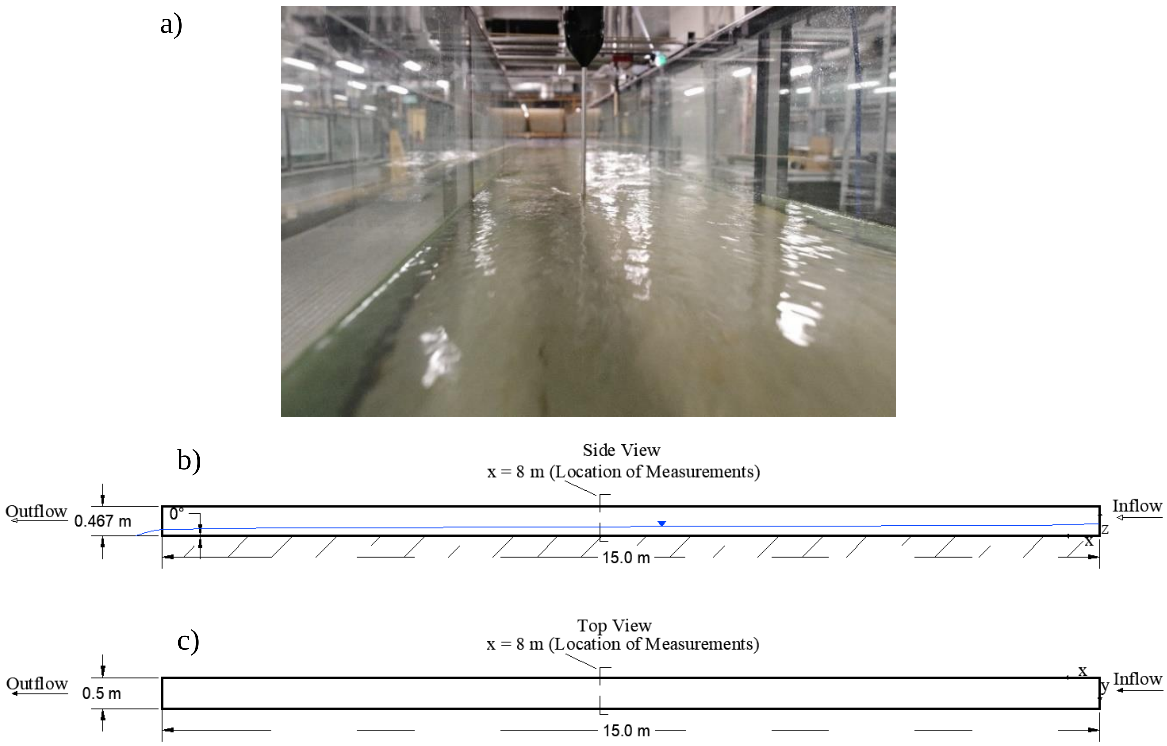


**Figure 3. Experimental facility and instrumentation at the University of Queensland. a) Flow conditions: Q = 0.0556 m$^3$/s, d = 0.144 m, flow direction from foreground to background at x = 8 m, with the acoustic Doppler velocimeter (ADV) in operation. b) Longitudinal sketch of the channel with flow direction from right to left. c) Top view of the channel**

The flow rate was recorded using a Venturi meter placed on the pipeline coming from the head tank. The meter was designed based upon (British Standard 1943) and built at the University of Queensland. The error of the discharge was less than 2%. The centreline water depth was recorded with a pointer gauge, with an accuracy of ±0.5 mm. The water velocities were measured with a Dwyer® 166 Series Prandtl-Pitot tube, with the opening parallel to the direction of flow and a Nortek™ Vectrino+ acoustic Doppler velocimeter (ADV), equipped with a side-looking head. The Prandtl-Pitot tube consisted of a Ø3.3 mm stainless steel tube, a hemispherical total head tapping (Ø = 1.19 mm) and four equally spaced static head tappings (Ø = 0.51 mm) at 25.4 mm behind the tip. The ADV signal was sampled at 200 Hz for 180 s at each location. All ADV signal data were post-processed to remove erroneous data and spikes. Data with an average correlation of less than 60% and an average signal-to-noise ratio (SNR) less than 5 dB were removed, and the signal was "despiked" using a phase-space thresholding technique (Goring and Nikora 2002; Wahl 2003). The experimental flow conditions were documented with a dSLR camera Pentax™ K-3iii for a high-resolution photographic record.

During this study, visual and free-surface observations were carried out for flow rates 0.029 m$^3$/s < Q < 0.100 m$^3$/s, and detailed velocity measurements were performed for Q = 0.0556 m$^3$/s at a longitudinal distance of 8 m from the start of the channel (x=8m). For a given flow rate, a total of 11 vertical profiles with a total of 385 data points were recorded and analysed for ADV measurement, and 9 vertical profiles with a total of 225 data points for pitot tube measurement. For pitot tube measurement, the vertical profiles were located at y = 0.0016 m, 0.03 m, 0.165 m, 0.25 m, 0.335 m, 0.435 m, 0.47 m, 0.49 m and 0.4984 m. The vertical profiles for ADV measurement were located at similar locations as the pitot tube measurement, with some additional profiles at y = 0.01 m, 0.065 m and the sidewall measurements were carried out at y=0.005 m and 0.495 m, a maximum of 5 mm from the wall due to the limitation of ADV in measuring points near the boundaries. y is the transverse distance from the right side of the channel, looking downstream, and y = 0.5 m corresponded to the left side of the channel. Careful observations and selections of the traverse locations were made to ensure the quality and the validity of the data. Table 1 details the flow conditions for three discharges: Q = 0.029 $m^3/s$, 0.0556 $m^3/s$ and 0.100 $m^3/s$.

**Table 1. Bed slope, Reynolds number and aspect ratio of the channel for all discharges involved in the detailed flow investigations, Q = 0.029 $m^3/s$, 0.0556 $m^3/s$ and 0.100 $m^3/s$**

| Bed slope, θ (°) | Width, B (m) | Discharge ($m^3/s$) | Depth, d (m) | Re x=8m | Fr | B/d at x=8m | Comment |
|---|---|---|---|---|---|---|---|
| 0 | 0.50 | 0.0290 | 0.099 | 1.7 E+05 | 0.59 | 5.05 | Smooth Channel |
| | | 0.0556 | 0.144 | 2.8 E+05 | 0.65 | 3.47 | |
| | | 0.1000 | 0.207 | 4.3 E+05 | 0.68 | 2.42 | |

## RESULTS

For all flow conditions, the open channel flow was subcritical, with Froude numbers less than unity. All flows were turbulent since Re>10,000 and the flow conditions lie between smooth and fully-rough turbulent flow.. The water level across the channel breadth was uniform. The bed slope was zero, and the depth was larger than the critical depth. The free surface profiles for all the discharges under this study were categorised as a H2 profile (Henderson 1966; Chanson 2004). The free surface measurements were compared to the integration of the backwater equation, assuming a constant equivalent sand roughness height, $k_s$, in the fully developed flow region. The Darcy-Weisbach friction factor f and roughness height $k_s$ were estimated based on the best data fit. For the present flow conditions, i.e. 0.029 $m^3/s$ < Q < 0.100 $m^3/s$, f and $k_s$ decreased from 0.0264 to 0.0216 and 0.0008 m to 0.0006 m respectively as the water discharge and Reynolds number increased. The trend in terms of Darcy-Weisbach friction factor versus Reynolds number was in agreement to the Karman-Nikuradse formula for smooth turbulent flow.

Figure 4 shows a typical contour map of time-averaged longitudinal velocity in the channel for a discharge Q = 0.0556 $m^3/s$. The boundary velocity was set to zero in accordance to the no-slip condition. The bulk of the flow cross-section area corresponded to large time-averaged longitudinal velocities, with maximum velocity $V_{max}/V_{mean}$ =1.09, with the bulk velocity $V_{mean}$ = Q/A, Q is the volume flow rate and A is the flow cross-section area. A slight assymmetrical flow condition in the cross-section was observed for the time-averaged longitudinal velocity, which could be due to the flow condition when water enters the channel on the upstream, reflecting and implying a similar flow that could be observed in a real site. As the friction along the boundaries induced from momentum transfer from the high-velocity regions, the longitudinal velocity was reduced in the vicinity of the invert and sidewalls. Several regions of low velocities (i.e. LVZs) were seen in the bottom corners and next to the sidewalls of the channel (Fig. 4).

The bottom corners played a key role of secondary currents because a transverse flow was directed towards the corner as a direct result of turbulent shear stress gradients normal to the edge bi-sector (Prandtl 1952; Gessner 1973). The secondary current map is shown in Figure 5 for Q = 0.0556 $m^3/s$. The velocities of the secondary currents at the channel centreline were near zero. For each side of the channel, the current was circulating towards the wall from the centreline, forming two vortical cells typical of Prandtl's second kind. The data indicated some secondary current magnitudes, i.e. $(V_y^2+V_z^2)^{1/2}$, with a median value of 0.051 m/s and 90% percentile of 0.34 m/s, corresponding respectively to 6.1% and 40% of the maximum velocity $V_{max}$. A strong horizontal flow, i.e. $|V_y| > 0$, occured near the free surface, as previously reported (Nezu and Rodi 1985). A downward flow motion $V_z < 0$ was observed next to both sidewalls.

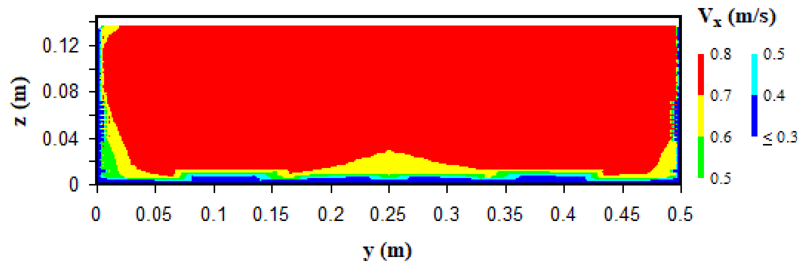


**Figure 4. Contour map of time-averaged longitudinal velocity, $V_x$, for Q = 0.0556 m$^3$/s**

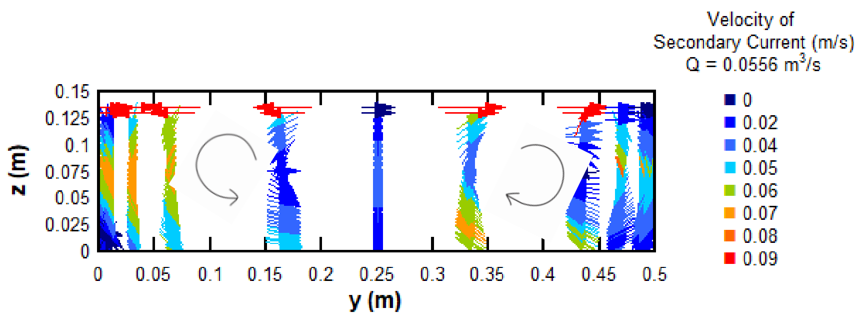


**Figure 5. Velocity vector field of secondary current obtained from the measured $V_y$ and $V_z$, for Q = 0.0556 m$^3$/s, with the colour codes as the magnitude of the secondary current**

In the time-averaged velocity field of the turbulent flow, a component derives from the extra apparent stress $Re_{xx} = \overline{\rho v_x{}^2}$ normal to the face dydz of a small control volume (Bradshaw 1971). Similarly, there are normal stresses $\overline{\rho v_y{}^2}$ and $\overline{\rho v_z{}^2}$ in the y and z directions. Tangential stresses that contribute to an extra mean shear stress on the face dxdy, dxdz and dydz are denoted $Re_{xy} = \overline{\rho v_x v_y}$, $Re_{xz} = \overline{\rho v_x v_z}$ and $Re_{yz} = \overline{\rho v_y v_z}$ respectively. These extra turbulent stresses produced by the fluctuating motions are named as the turbulent Reynolds stresses (Bradshaw 1971). The measurement and analysis of Reynolds stresses are essential to locate the regions of high and low turbulence in the channel. For this study, the velocity signal outputs were analysed to estimate the time-averaged normal and tangential Reynolds stresses. The time-averaged Reynolds stresses $Re_{xx}$, $Re_{xy}$ ad $Re_{xz}$ are plotted in Figures 6a, 6b and 6c, as these contributed dominantly to the secondary current motion. Figure 6a is the contour map of the Reynolds stress $Re_{xx}$ in the longitudinal direction normal to the control volume face dydz. The data showed higher longitudinal turbulent stresses next to the sidewalls and in the bottom corners, with lower turbulent stresses in the central regions of the channel. The contour map of the tangential stresses with the longitudinal velocity component, $Re_{xy}$ ad $Re_{xz}$, are shown in Figure 6b and 6c. The data indicated higher positive Reynolds stresses in the x-y plane next to the left sidewall whereas higher negative Reynolds stresses were observed next to the right sidewall. Similarly, Figure 6c shows the higher positive Reynolds stresses $Re_{xz}$ in the x-z plane next to the left side wall, with higher negative Reynolds stresses next to the right side wall. Altogether, the present data demonstrated that the regions with the highest turbulent stresses were located next to the channel boundaries, with the lowest turbulent stresses about the channel centre, where the velocities were the largest. A similar observation was reported by Hockley et al. (2014).

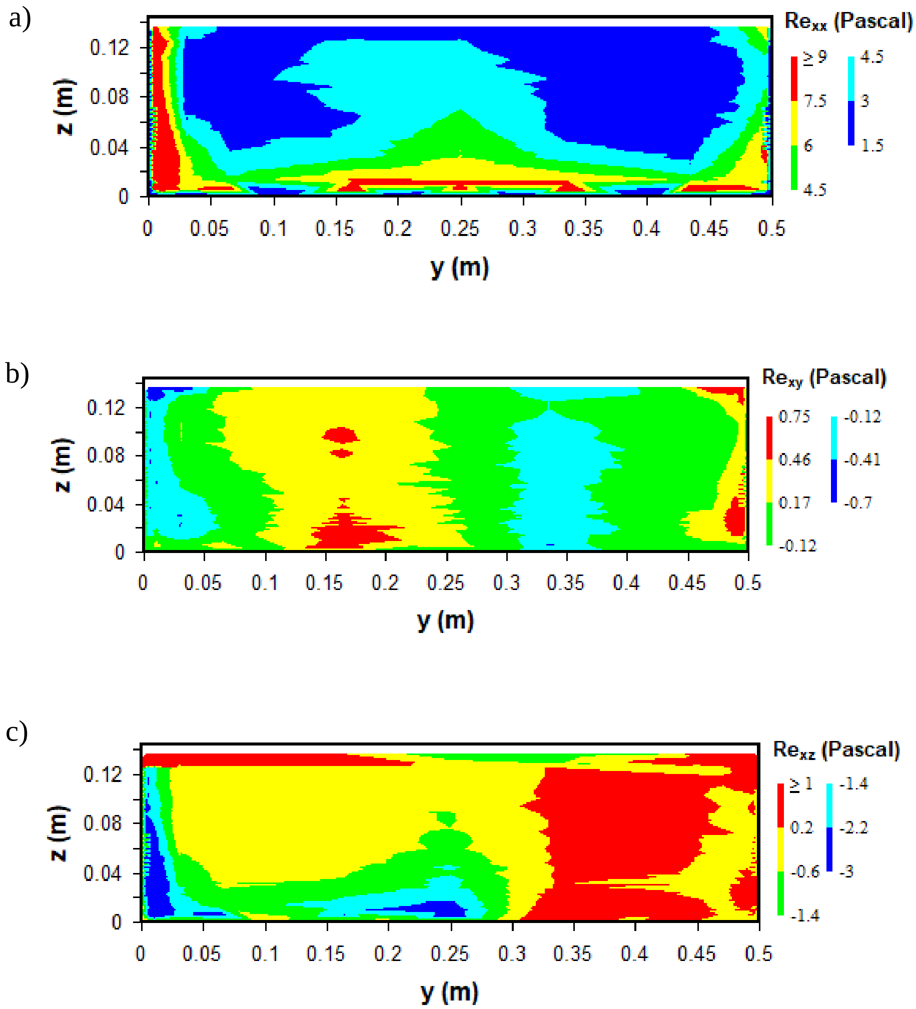


**Figure 6 Contour map of time-averaged Reynolds stresses for Q = 0.0556 m$^3$/s, d = 0.144 m. a) Reynolds stress $Re_{xx}$ in the longitudinal direction. b) Reynolds stress $Re_{xy}$ in the x-y plane. c) Reynolds stress $Re_{xy}$ in the x-z plane**

From the time-averaged longitudinal velocity contour plot, the relative size of LVZs were determined for 30%, 50%, 70%, 85% and 100% of the bulk velocity $V_{mean}$. Basically, the relative LVZ area increased with the percentage of bulk velocity (Figure 7). Such a relationship is relevant to various stakeholders to identify the percentage of LVZ area for a wide range of dicharges and channel aspect ratio. The present data were further compared to previous experiment data (Leng and Chanson 2020b) in Figure 7. The comparison showed a similar data trend. The current data were scattered about the mean trend proposed by Leng and Chanson (2020b). The differences were the largest for 85% and 100% of the bulk velocity, with a closer agreement at lower relative velocities which could be due to the different aspect ratio, channel roughness and different flow conditions and instrumentations.

In design practice, the longitudinal velocity is often the determining factor for upstream fish passage in culvert barrel. Three small-bodied Australian and New Zealand native fish (i.e.length < 120 mm) were selected to assess the traversability of the culvert barrel channel under Q = 0.0556 m$^3$/s, based on the present longitudinal velocity data and published critical swimming speed (Table 2). The critical swimming speed ($U_{crit}$) is mainly used to assess the prolonged swimming performance, interpolated from its final swimming performance as the maximum velocity the fish can keep swimming (Farrell, 2007). For each relative critical swimming speed $U_{crit}/V_{mean}$, the relative LVZ area was interpolated in

Figure 7. A further physical constraint is the dimensions of the fish, in particular its height, relative to the LVZ dimensions in the channel. For the selected fish species, the body height was larger than 10 mm, when the height of LVZ based on their respective $U_{crit}/V_{mean}$ ratio was less than 4 mm. Aside from height consideration, fishes need additional spaces to manoeuvre. The LVZ size in the bottom corner may be characterised by its diagonal length DL, with a proposed minimum requirement of 35 mm (Chanson and Leng 2020). Altogether, the present detailed data set suggested that the single-box culvert barrel channel under Q = 0.0556 $m^3/s$ would not be passable for all the three species.

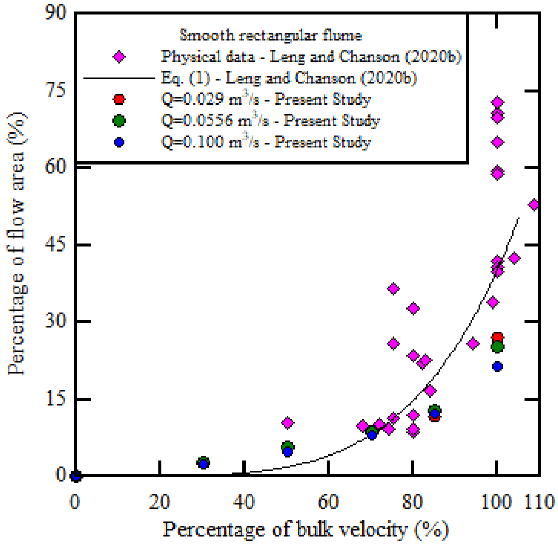


**Figure 7. Dimensionless relationship between the percentage of bulk velocity and the percentage of flow area. Comparison between present data (Q = 0.029 $m^3/s$, 0.0556 $m^3/s$ & 0.100 $m^3/s$) highlighted in red, green and blue circular symbols and data from Leng and Chanson (2020b)**

## DISCUSSION

The literature broadly acknowledged that fish prefer to swim upstream next to the culvert barrel sidewall, irrespective of the species (Katopodis and Gervais 2016; Cabonce et al. 2019; Miles et al. 2021; Chanson and Leng 2020). In contrast, a few studies mentioned that fish prefer swimming in regions with lesser turbulence (Hockley et al. 2014; Marsden et al. 2018; Muhawenimana et al. 2019), although low velocity and low turbulence conditions are not the first preferred swimming location, e.g. for juvenile Atlantic salmon (Enders et al. 2005). The present study confirmed that some higher turbulence was observed next the sidewalls, in the low velocity zones and preferred swimming zones. The finding is consistent with Cotel et al. (2006) stating that the lowest turbulence intensity are regions with the fastest current. Studies showed that some fish species can sustain very high turbulent stresses, e.g. Iberian barbel with minimum total length of 150 mm could occupy areas with Reynolds stresses up to 60 Pa (Silva et al. 2011), while hydrid bass, rainbow trout and atlantic salmon can be exposed to Reynolds shear stress higher than 50 Pa without significant mortality, even when exposed for more than 48 hours (Odeh et al. 2002). Hence, there is also a need to assess and consider the Reynolds stresses each fish species can withstand when developing the design guideline for fish passage in a box culvert.

Noteworthily, the literature highlighted a lack of standardised testing methods for the fish prolonged swimming speed (Kemp 2012; Katopodis and Gervais 2016). This was highlighted in the swimming data reported in Table 2. Hurst et al. (2007) utilised the ramp velocity test to obtain $U_{crit}$ and the fish was judged to fatigue when they were swept against the mesh. Svozil et al. (2020) used a 25 cm long, 7.1×5.2 $cm^2$ cross-section recirculating swim tunnel for the testing of critical swim speed. The authors defined fish fatigue when the fish was swept against the mesh and unable to resume swimming for 30 s. Nikora et al. (2003) employed a recirculating flume for critical speed test with rough and smooth channel. They assumed fish fatigue when the fish became impinged at the back screen for more than 30 s and refused to swim despite tapping and temporary flow reduction. Simply, the differences in defining fatigue and its thresholds can influence the performance measurement, such as when incidental contacts occurs in an automated system. Katopodis and Gervais (2016) argued that any design criteria based on fish swimming to exhaustion is not realistic. In summary, there is an urgent need to standardise the methodology for each fish test and develop other pragmatic parameters to quantify the fish swimming speed volitionally for a realistic design of fish passage structures.

**Table 2. Fish accessibility in the culvert with flow of Q = 0.0556 $m^3/s$, based on the critical swimming speed of fish species and longitudinal velocity field in the channel**

| Fish Species (Scientific Name) | Fish Species (Common Names) | Fish Length, L (mm) | Mean fish height and width, H and W (mm×mm) | Mean critical swim speed, $U_{crit}$ (m/s) | Percentage of Bulk Velocity (%) | Percentage of LVZ area in culvert for passage (%) | Diagonal Length, DL (mm) | Height of LVZ (mm) |
|---|---|---|---|---|---|---|---|---|
| *Retropinna semoni* | Australian Smelt | 25 – 57 (1) | 14.0 × 4.5 (4) | 0.466 (1) | 59.6 | 7.08 | 11.0 | 4.0 |
| *Melanotaenia duboulayi* | Crimson Spotted Rainbow fish | 48.8 ± 1.8 (2) | 12.6 (5) (H) | 0.44 (2) | 57.0 | 6.67 | 10.8 | 4.0 |
| *Galaxias maculatus* | Common Galaxias (Inanga – New Zealand) | 48 ± 2.5 to 91.8 ± 10.3 (3) | 10.0 × 8.0 (3) | 0.19 – 0.36 (3) | 35.6 | 3.40 | 10.6 | 2.5 |

(1) Standard Length (SL) of fish and the tested mean critical swimming speed (Svozil et al. 2020); (2) Mean Total Length of fish and the tested mean critical swimming speed (Hurst et al. 2007); (3) Fork Length (LF), height of fish and the tested mean critical swimming speed (Nikora et al. 2003); (4) Height of fish (Hendry et al. 2002) with similar body shape with Svozil et al. (2020); (5) Body height of fish (McGuigan et al. 2003) with similar body length as Hurst et al. (2007).

## CONCLUSION

Some new research was carried out with the aim of developing fish friendly box culverts without altering the design capacity. Near-full-scale experiments were carried out in a box culvert barrel, 0.5 m wide and 15 m long. Detailed velocity and turbulence measurements were undertaken for a range of flow conditions, likely to correspond to less-than-design flood events, during which fish may attempt to traverse the structure. In standard box culvert barrel, the turbulent Reynolds stresses were the highest next the boundaries of the channel and in the bottom corners. The high Reynolds stresses and vigorous secondary current motion of Prandtl's second kind favoured the development of large longitudinal vortices. They were also conducive of low velocity zones along the culvert barrel boundaries, and such regions are the preferential swimming zone of fish traversing upstream for a culvert structure. This experiment utilised PVC and glass for the channel bed and sidewall, which is equivalent to a relatively new smooth concrete. For older concrete channel, the boundary roughness $k_s$ value would be higher and a larger LVZ area would be expected for an identical discharge.

While the literature covers many guidelines focused primarily on the longitudinal velocity as the basis of fish passage design, this study demonstrated that a sound understanding of turbulence typology is essential to solve the conundrum of fish passage at road-crossings. Future design guideline should incorporate some form turbulence control for an optimum sizing of the culvert barrel.

## ACKNOWLEDGEMENTS

The authors acknowledge the technical assistance for Jason Van Der Gevel and Stewart Matthews (The University of of Queensland). Hui Ling Wong acknowledges the financial support of the Research

Training Program (RTP), funded by the Commonwealth Government of Australia and the University of Queensland.

In line with recommendations of the International Committee on Publication Ethics (COPE) and the Office of the Commonwealth Ombudsman (Australia), Hubert Chanson declares a major conflict of interest with Craig E. Franklin (The University of Queensland).

## REFERENCES

Anderson, G.B., Freeman, M.C., Freeman, B.J., Straight, C.A., Hagler, M.M. & Peterson, J.T. (2012) Dealing with uncertainty when assessing fish passage through culvert road crossings. *Environmental Management*, 50, 462–477.

Baumgartner, L.J., Marsden, T., Singhanouvoung, D., Phonekhampheng, O., Stuart, I.G., & Thorncraft, G. (2012) Using an experimental in situ fishway to provide key design criteria for lateral fish passage in tropical rivers: a case study from the Mekong River, Central Lao PDR. *River Research and Applications*, 28, 1217-1229.

Behlke, C.E., Kane, D.L., McLeen, R.F. & Travis, M.T. (1991) Fundamentals of culvert design for passage of weak-swimming fish. *Report FHW A-AK-RD-90–10*, Department of Transportation and Public Facilities, State of Alaska, Fairbanks, USA. 178 pages.

Blank, M.D. (2008) Advanced Studies of Fish Passage through Culverts: 1-D and 3-D Hydraulic Modelling of Velocity, Fish Energy Expenditure, and a New Barrier Assessment Method. *Ph.D. Thesis*, Montana State University, Department of Civil Engineering. 231 pages.

Bradshaw. P. (1971) *An Introduction to Turbulence and Its Measurement*. Elsevier Science & Technology, 1971. 218 pages. (ISBN: 0080166202, 9780080166209).

British Standard (1943) Flow Measurement. *British Standard Code BS 1042:1943*, British Standard Institution, London.

Cabonce, J., Fernando, R., Wang, H. & Chanson, H. (2019) Using small triangular baffles to facilitate upstream fish passage in standard box culverts. *Environmental Fluid Mechanics*, 19(1), 157–179 (DOI: 10.1007/s10652-018-9604-x).

Cahoon, J.E., McMahon, T., Solcz, A., Blank, M.D. & Stein, O. (2007) Fish passage in Montana culverts: Phase II: Passage goals. *Report FHWA/MT-07–010/8181*, Montana Department of Transportation and US Department of Transportation, Federal Highway Administration. 61 pages.

Chanson, H. (2004) *The Hydraulics of Open Channel Flow: An Introduction*. Butterworth-Heinemann, 2nd edition, Oxford, UK, 630 pages.

Chanson, H. (2019) Utilising the boundary layer to help restore the connectivity of fish habitats and populations: An engineering discussion. *Ecological Engineering*, 141, Paper 105613, 5 pages (DOI: 10.1016/j.ecoleng.2019.105613).

Chanson, H., & Leng, X. (2020) *Fish Swimming in Turbulent Waters. Hydraulics Guidelines to assist Upstream Fish Passage in Box Culverts*. CRC Press, Taylor and Francis Group, Leiden, The Netherlands, 202 pages & 19 video movies (DOI: 10.1201/9781003029694).

Cotel, A., Webb, P.W., & Tritico, H. (2006) Do Brown Trout Choose Locations with Reduced Turbulence?, *Transactions of the American Fisheries Society*, 135:3, 610-619.

Enders, E., Buffin-Bélanger, T.,Boisclair, D. & Roy, AG. (2005) The feeding behaviour of juvenile Atlantic salmon in relation to turbulent flow. *Journal of Fish Biology*. 66(1), 242-253.

Farrell, A. P. (2007). Cardiorespiratory performance during prolonged swimming tests with salmonids: A perspective on temperature effects and potential analytical pitfalls. In Philosophical Transactions of the Royal Society B: Biological Sciences (Vol. 362, Issue 1487, pp. 2017–2030). Royal Society.

(DOI:doi.org/10.1098/rstb.2007.2111).

Gessner, F.B. (1973) The Origin of Secondary Flow in Turbulent Flow along a Corner. *Journal of Fluid Mechanics*, Vol. 58, Part 1, pp. 1-25.

Henderson, F.M. (1966) *Open Channel Flow*. MacMillan Company, New York, USA.

Hendry, A. P., Taylor, E. B., & McPhail, J. D. (2002) Adaptive Divergence and the Balance between Selection and Gene Flow: Lake and Stream Stickleback in the Misty System. *Evolution*, 56(6), 1199-1216.

Hockley F. A., Wilson C. A. M. E., Brew A. and Cable J. (2014) Fish responses to flow velocity and turbulence in relation to size, sex and parasite load. *J. R. Soc. Interface*. 11(91), 20130814, 11pp.

Hurst, T. P., Kay, B. H., Ryan, P. A., & Brown, M. D. (2007) Sublethal effects of mosquito larvicides on swimming performance of larvivorous fish *Melanotaenia duboulayi* (Atheriniformes: Melanotaeniidae). *Journal of economic entomology*, 100(1), 61-65 (DOI: 10.1093/jee/100.1.61).

Jensen, K.M. (2014) Velocity Reduction Factors in Near Boundary Flow and the Effect on Fish Passage through Culverts. *Master of Science Thesis*, Brigham Young University, USA, 44 pages.

Katopodis, C. and Gervais, R. (2016) Fish swimming performance database and analyses. *DFO Can. Sci. Advis. Sec. Res. Doc. 2016/002*. vi + 550 pages.

Kemp, P. (2012) Bridging the gap between fish behaviour, performance and hydrodynamics: An ecohydraulics approach to fish passage research. *River Research and Applications*, 28, 403–406.

Leng, X. & Chanson, H. (2020) Hybrid modelling of low velocity zones in box culverts to assist fish passage: Why simple is better! *River Research and Applications*, 36(9), Review Paper, 1765-1777 (DOI: 10.1002/rra.3710).

Leng, X., and Chanson, H. (2020b) Hybrid Modelling of Low Velocity Zones in Box Culverts to Assist Upstream Fish Passage. *Environmental Fluid Mechanics*, 20(2), 415-432 (DOI: 10.1007/s10652-019-09700-1).

Mallen-Cooper, M. (1996) Fishways and Freshwater Migration in South-Eastern Australia. *Ph.D. thesis*, University of Technology of Sydney, Faculty of Science, 42 pages.

Marsden, T. et. al. (2018) Stung Pursat Barrage Fishway: proposed design criteria and concept. *Australasian Fish Passage Services Pty Ltd*, 21 pages.

McGuigan, K., Franklin, C. E., Moritz, C., & Blows, M. W. (2003) Adaptation of rainbow fish to lake and stream habitats. *Evolution; international journal of organic evolution*, 57(1), 104-118.

Miles, J., Vowles, A.S.& Kemp, P.S. (2021) The response of common minnows, Phoxinus phoxinus, to visual cues under flowing and static water conditions. *Animal Behaviour*. 179. 289-296.

Muhawenimana, V., Wilson, C. A. M.E., Ouro, P., & Cable, J. (2019) Spanwise cylinder wake hydrodynamics and fish behavior. *Water Resources Research*, 55, 8569–8582.

Nezu, I., and Rodi, W. (1985) Experimental Study on Secondary Currents in Open Channel Flow. *Proceedings 21st IAHR Biennial Congress*, Melbourne, Australia, pp. 114-119.

Nikora, V.I., Aberle, J., Biggs, B.J.F., Jowett, I.G., Sykes, J.R.E. (2003) Effects of fish size, time-to-fatigue and turbulence on swimming performance: A case study of Galaxias maculatus. *Journal of Fish Biology*. 63, 1365-1382 (DOI: 10.1111/j.1095-8649.2003.00241.x).

Odeh, M., Noreika, J.F., Haro, A., Maynard, A., & Castro-Santos, T. (2002) Evaluation of the Effects of Turbulence on the Behavior of Migratory Fish. *Report to the Bonneville Power Administration*, Contract no. 00000022, Project no. 200005700 (BPA Report DOE/BP-00000022-1).

Olsen, A. & Tullis, B. (2013) Laboratory study of fish passage and discharge capacity in slip-lined, baffled culverts. *Journal of Hydraulic Engineering*, ASCE, 139(4), 424-432.

Prandtl, L. (1952) *Essentials of Fluid Dynamics with Applications to Hydraulics, Aeronautics, Meteorology and Other Subjects*. Blackie & Son, London, UK, 452 pages.

Sailema, C., Freire, R., Chanson, H. & Zhang, G. (2020) Modelling small ventilated corner baffles for box culvert barrel. *Environmental Fluid Mechanics*, Springer, 20(2), 433-457 (DOI: 10.1007/s10652-019-09680-2).

Silva, A.T, Santos, J.M., Ferreira M.T., Pinheiro, A.N., & Katopodis, C. (2011) Effects of water velocity and turbulence on the behaviour of Iberian barbel (Luciobarbus bocagei, Steindachner 1864) in an experimental pool-type fishway. *River Research and Applications*. 44. 360-373.

Svozil, D.P., Baumgartner, L.J., Fulton, C.J., Kopf, R.K., Watts, R.J., (2020) Morphological predictors of swimming speed performance in river and reservoir populations of Australian smelt Retropinna semoni. *Journal of Fish Biology*. 97 (6), 1632-1643 (DOI: 10.1111/jfb.14494).

Wang, H., Chanson, H., Kern, P. & Franklin, C. (2016) Culvert hydrodynamics to enhance upstream fish passage: Fish response to turbulence. *Proceedings of 20th Australasian Fluid Mechanics Conference*, Australasian Fluid Mechanics Society, Perth WA, Australia, 5–8 December, Ivey, G., Zhou, T., Jones, N. & Draper, S. (eds.), Paper 682, 4 pages.

Warren, M.L., Jr. & Pardew, M.G. (1998) Road crossings as barriers to small-stream fish movement. *Transactions of the American Fisheries Society*, 127, 637–644.

## BIOGRAPHY

Hui Ling Wong (GradIEAust) is a Ph.D. research student in hydraulic engineering at the University of Queensland. She graduated with MEng Civil Engineering from the University of Nottingham with First Class Honours in 2022. She has been working in the UQ AEB Hydraulics Laboratory since 2023 under the supervision of Professor Hubert Chanson. She has published several papers mainly on coastal reservoirs and river basin management. Her research interests include sustainable development, ecohydraulics, coastal hydraulics, turbulence and open channel flow.

Hubert Chanson is Professor of Civil Engineering at the University of Queensland, where he has been since 1990, having previously enjoyed an industrial career for six years. His main field of expertise is environmental fluid mechanics and hydraulic engineering, both in terms of theoretical fundamentals, physical and numerical modelling. He leads a group of 5-8 researchers, largely targeting flows around hydraulic structures, two-phase (gas-liquid and solid-liquid) free-surface flows, turbulence in steady and unsteady open channel flows, using computation, lab-scale experiments, field work and analysis. He has published over 1,350 peer reviewed publications including two dozen of books. He serves on the editorial boards of International Journal of Multiphase Flow, Flow Measurement and Instrumentation, and Environmental Fluid Mechanics, the latter of which he is currently a senior Editor. His Youtube channel is: {https://www.youtube.com/@Hubert_Chanson}.